RSC Advances

COMMUNICATION

Cite this: *RSC Adv.*, 2014, **4**, 32726

Received 3rd April 2014
Accepted 11th July 2014

DOI: 10.1039/c4ra06005a

www.rsc.org/advances

Triple excitation with dual emission in paramagnetic ZnO:Er^{3+} nanocrystals

Swati Bishnoi, Naveen Khichar, Rupali Das, Vineet Kumar, R. K. Kotnala and Santa Chawla*

ZnO nanocrystals have been made excitable under UV as well as near and far infrared (IR) wavelengths (980 nm, 1550 nm) through doping of rare earth ion Er^{3+} thus making it a triple excitation nanophosphor. Whereas the visible emission under UV is broad due to intrinsic donor acceptor pair recombination, the sharp green and red emission peaks under IR are characteristic of f–f transitions of the Er^{3+} ion. Thus both down and upconversion fluorescence in ZnO could be realised through doping of rare earth ion Er^{3+} that also makes ZnO:Er^{3+} nanocrystals paramagnetic. To the best of our knowledge we are reporting upconversion at 1550 nm in ZnO:Er^{3+} for the first time.

Introduction

Rare earth (RE) doping in semiconductor nanocrystals makes them a special class of materials where semiconductor characteristics can be combined with fundamental light emitting properties of RE ions that include optical conversion of IR photons to shorter wavelength photons[1–4] for RE ions such as Er^{3+}, Ho^{3+}, Tm^{3+}. ZnO is a unique multifunctional semiconductor due to its direct band gap (3.37 eV) that can host 4f levels of RE ions[7–9] to exhibit excellent optical properties,[5,6] anisotropic structure and spontaneous polarization that render ZnO properties such as lasing, piezoelectric and ferroelectric behaviour[10,11] and also dilute magnetism with appropriate doping.[12,13] Among all RE ions, Er^{3+} ion is most suitable for upconversion of IR photons with wavelength 1 μm and longer due to its level spacing of ground $^4I_{15/2}$ level and lowest excitable $^4I_{13/2}$ and $^4I_{11/2}$ levels. Er^{3+} ions based upconversion has been already reported by many researchers.[14–17] Er^{3+} shows efficient upconversion emissions in green and red spectral ranges. Also Er^{3+} ions can be pumped by low cost diode laser. In Er^{3+} ions doped semiconductor there occurs a series of non-radiative and radiative decay mechanism which results in generation of photons having energy lower than the excitation photon.[18,19] Er^{3+} ion acts as a good activator for solid state laser in IR and visible region because of its characteristics of abundant energy level structure. The low phonon energy and proper oxygen coordination around Er^{3+} ions make ZnO suitable for upconversion luminescence process.[20]Also ZnO can provide proper environment for the coexistence of Er and O, which results in ErO_6 complex formation, this complex can optically activate Er^{3+} ions. So far in Er^{3+} doped ZnO samples upconversion at 980 nm excitation has been reported.[21,22] but down conversion (UV excitation) has been explored less.[23] The UC luminescence spectra of Er^{3+}-doped ZBLAN-type glass under IR excitation at 1520 nm,[24] ZrO_2:Er under 1438 nm,[25] oxysulfide, M_2O_2S (M = Y, Gd, La) phosphors[26] under 1550 nm excitation and Er:$LiNbO_3$ crystal under 1550 nm excitation[27] have been reported.

In this paper we are reporting, the upconversion phenomenon in ZnO:Er^{3+} sample under 1550 nm excitation for the first time (to the best of our knowledge). At the same time we have also shown the results of upconversion under 980 nm excitation and down conversion under 375 nm excitation. So here we are reporting triple excitation (370 nm, 980 nm and 1550 nm) and dual emission in Er^{3+} doped ZnO. Triple excitation capability that encompass solar UV and IR region and visible emission covering the maximum spectral response region of solar cells make them potential nanophosphor for solar spectrum conversion. The present study shows that Er^{3+} doping in ZnO nanocrystals not only make them triple excitation nanophosphor but also makes them paramagnetic thus making them bi-functional - DC and dual wavelength UC fluorescent, magnetic semiconductor. A bi-functional non toxic semiconductor such as ZnO:Er^{3+}could have special advantage for application in biological systems due to negligible autofluorescence and photo bleaching with IR excitation. The synthesis, structural, luminescence and magnetic properties of ZnO doped with Er^{3+} ions have been described.

Results and discussion

The prepared ZnO:Er^{3+} white powder exhibited wurtzite hexagonal phase of ZnO (JCPDS Card no. 36-1451) as shown in Fig. 1a

Luminescent Materials Group, National Physical Laboratory, Dr. K. S. Krishnan Road, New Delhi-110012, India. E-mail: santa@nplindia.org; Fax: +91 11 45609310; Tel: +91 11 45609242

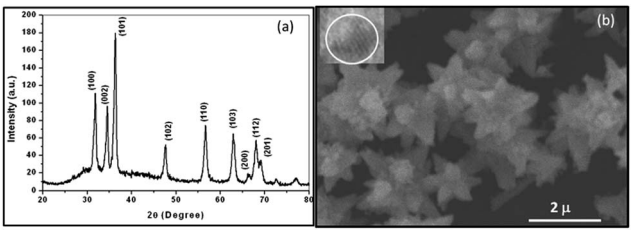

Fig. 1 (a) XRD spectra and (b) SEM micrograph of ZnO:Er^{3+} powder sample, insert shows HRTEM image of a single nanocrystal.

with sharp peaks clearly suggesting that the product was well crystallized and that Er^{3+} doping does not affect the host ZnO structure. SEM and HRTEM studies of the synthesized Er^{3+} doped ZnO powder samples (Fig. 1b) revealed flower like hierarchical structure comprising individual nanoparticles of average diameter 5 nm (inset, Fig. 1b).

For photoluminescence (PL) spectroscopy and fluorescence mapping with confocal fluorescence microscope under sequential excitation of three diode lasers with wavelengths 375 nm, 980 nm and 1550 nm for realizing both down and up conversion properties of ZnO:Er^{3+} nanocrystals, a specific area of the sample was chosen under a 100× objective. The fluorescence images of the selected area (as marked in the optical image Fig. 2(iv)) and corresponding confocal PL spectra is shown under excitation of 375 nm UV laser (Fig. 2(i) and (v)), 980 nm IR laser (Fig. 2(ii) and (vi)) and 1550 nm IR laser (Fig. 2(iii) and (vii)). The emission under 375 nm laser excitation is very bright and the corresponding PL spectra show broad peaks at blue green (510 nm) and red (663 nm) arising due to donor acceptor pair recombination comprising native point defects as well as Er^{3+} donor centre as elucidated in the energy level diagram (Fig. 2(viii)). A comparison of optical image (area under green square in Fig. 2(iv)) and the fluorescence map of the marked area clearly elucidate the strong and near uniform fluorescence distribution suggesting that the ZnO:Er^{3+} nanocrystals are excellent spectral converters that can absorb UV and emit in the visible region spanning blue green to red. The excitation at 375 nm is across ZnO band gap. The native point defects responsible for PL emission in ZnO:Er^{3+} could be zinc vacancy centre (V_{Zn2+}) which act as acceptor centre which lie 0.3 eV (ref. 28) above ZnO valence band and have very low formation energy and favourable in oxygen rich synthesis conditions as in the present case. Charge compensation in ZnO doped with Er^{3+} would require that two Er^{3+} ions are substituted for three Zn^{2+} ions. For trivalent state of Er^{3+} dopant, overall charge neutrality in the lattice could be maintained either by creating one Zn^{2+} vacancy for incorporation of each two Er^{3+} ions or introducing one oxygen interstitial (O_i^{2-}) defect. Recombination of electrons from an intrinsic donor level to V_{Zn} acceptor centre give rise to blue green emission peak at 510 nm. In ZnO:Er^{3+}, the presence of zinc vacancies may increase as the substitution demands presence of vacancy in neighbouring position for charge compensation. The dopant Er^{3+} can act as a donor centre and recombination with V_{Zn} acceptor centre could give rise to broad red emission at 663 nm.

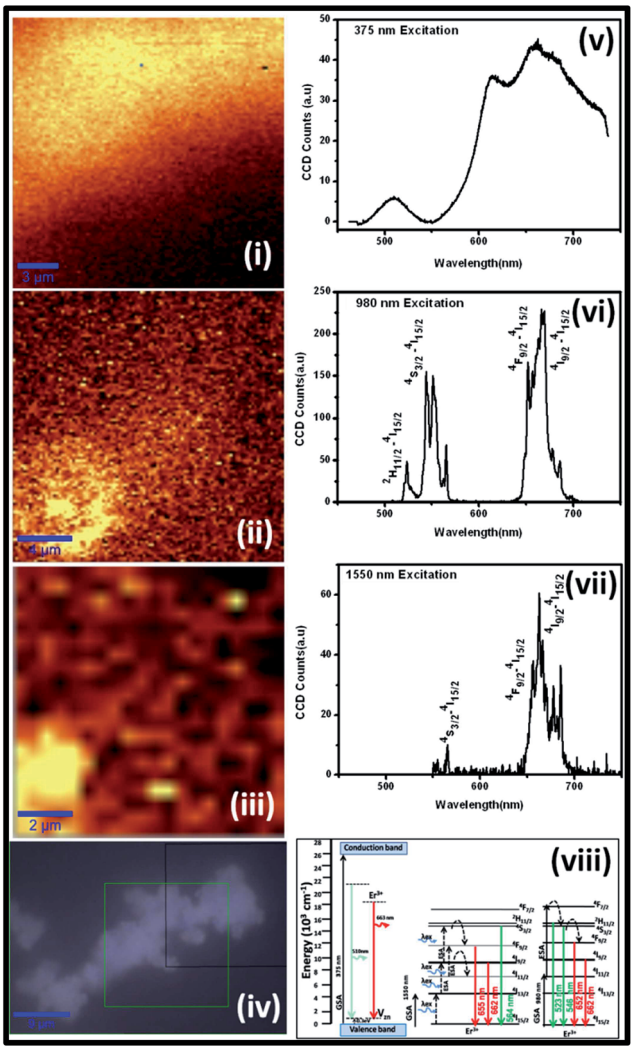

Fig. 2 Confocal fluorescence image and corresponding integrated photoluminescence spectra of ZnO:Er^{3+} nanocrystals under excitation of 375 nm (i) and (v); (ii) 980 nm (ii) and (vi); 1550 nm (iii) and (vii) laser; optical image (iv) with marked areas for which fluorescence image has been mapped and energy level diagram (viii) elucidation the DC and UC processes under three excitation wavelengths.

The confocal fluorescence map (corresponding to area under black square in the optical image Fig. 2(iv)) and corresponding PL emission spectra under illumination of 980 nm as well as 1550 nm lasers (Fig. 2(ii)–(vi)) clearly show that the upconversion photoluminescence occurs at both the wavelengths of excitation due to direct excitation of Er^{3+} ions from $^4I_{15/2}$–$^4I_{11/2}$ level and $^4I_{15/2}$–$^4I_{13/2}$ level respectively. Multiphoton absorption of IR photons leads to population of upper Er^{3+} levels and subsequent radiative emission in the visible range exhibits bright emission under 980 nm and 1550 nm excitation and corresponding UC emission spectra show that the spectral characteristics of UC emission remain identical under excitation of both IR lasers, though relative intensity of green and red emission differs. The green emission is due to transition $^2H_{11/2}$–$^4I_{15/2}$, $^4S_{3/2}$–$^4I_{15/2}$ levels and red emission is due to $^4I_{9/2}$–$^4I_{15/2}$, $^4F_{9/2}$–$^4I_{15/2}$ level transition of Er^{3+} ions. The

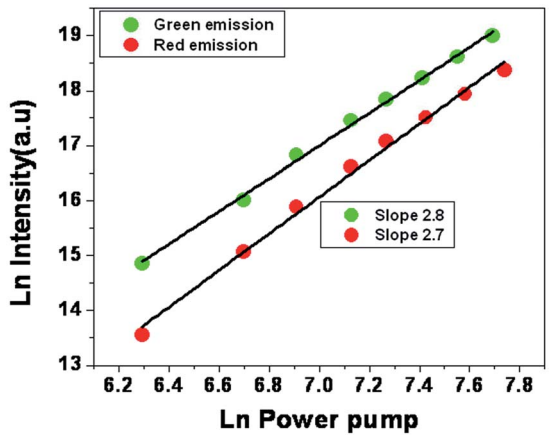

Fig. 3 Pump power plot at 980 nm excitation.

excitation and emission processes for both 980 nm and 1550 nm excitation is shown in the energy level diagram (Fig. 2(viii)).

The DC and UC fluorescence imaging and PL spectra described above clearly indicate that ZnO:Er^{3+} can be excited in three spectral ranges of UV, near IR (980 nm) and IR (1550 nm). The triple excitable ZnO:Er^{3+} thus exhibit dual mode luminescence emission characteristics.

Under 980 nm excitation, we have measured the dependence of UC emission intensity for both green and red emission with pump (excitation) laser power and the relationship is depicted in Fig. 3. It clearly shows that the upconversion is a two to three photon process.

The triple mode fluorescent ZnO:Er^{3+} is found to be paramagnetic down to 77 K as observed by continuously increasing magnetization with applied magnetic field (Fig. 4) without any hysteresis with maximum magnetization of 40 emu g^{-1} at room temperature (300 K) and 140 memu g^{-1} at 77 K at 4900 Gauss field. The samples were prepared with utmost caution to avoid any possible magnetic contamination and undoped ZnO prepared under the same conditions showed diamagnetic behaviour. Magnetism is introduced in ZnO due to doping with

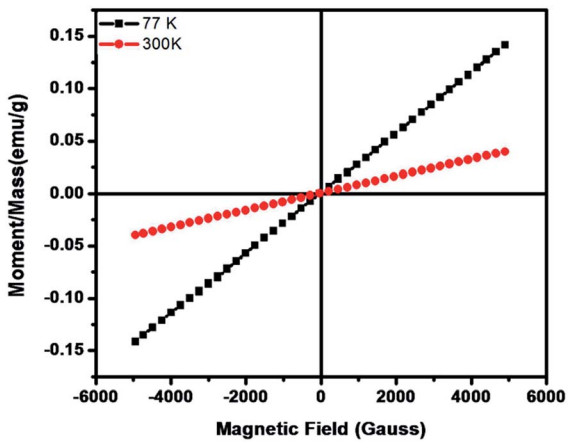

Fig. 4 Magnetization curve of Er^{3+} doped ZnO particles exhibiting paramagnetism.

rare earth Er^{3+} ion in which total number of 4f electrons is 11 and maximum number of unpaired electrons is 3. As f- electrons in rare earth ions are relatively loosely bound, they can interact with 2p electrons of the neighbouring oxygen atoms which mediate the magnetic interaction resulting into a long range ordering inducing paramagnetic behaviour in the nanocrystals. Such trivalent RE doped magnetism has also been observed in Ho^{3+} doped ZnO (ref. 29) and Er^{3+} doped SnO_2.[30] The conclusive evidence of bi-functionality in ZnO:Er^{3+} particles come from confocal fluorescence microscopy and magnetic *(B–H)* measurements that shows bright visible fluorescence and continuously increasing magnetization with increase in applied magnetic field without any hysteresis (Fig. 4).

Conclusions

We have demonstrated triple excitation (375 nm, 980 nm and 1550 nm) and dual emission behaviour in ZnO:Er^{3+} nanocrystals of average dimension 5–10 nm that form hierarchical nanoflowers. Upconversion phenomenon in ZnO:Er^{3+} nanocrystals at 1550 nm IR excitation is reported for the first time, to the best of our knowledge. The ZnO:Er^{3+} nanocrystals prepared through facile coprecipitation technique not only exhibit both down and up conversion fluorescence but also paramagnetic behaviour down to 77 K. The triple excitation range of ZnO:Er^{3+} nanocrystals cover the solar UV and IR region that remains unutilized by existing solar cells. As the visible emission under both UV and IR excitation cover the maximum spectral response region of solar cells, ZnO:Er^{3+} nanocrystals can be potential nanophosphor for solar spectrum conversion and when conjugated with silicon solar cell as a phosphor layer can enhance its efficiency. Another useful application of magnetic nanophosphor with triple mode excitation such as ZnO:Er^{3+}, could be in biological tracking.

Experimental

Materials

Trivalent lanthanum ion Er^{3+} (2 mole%) doped ZnO nanoparticles were synthesized by co-precipitation (CPP) method at room temperature with Er^{3+} as substitutional dopant in zinc position. Sub molar (0.027 M) aqueous solutions of precursors zinc acetate ($Zn[(CH)_3(COOH)]_2 \cdot 2H_2O$) Erbium nitrate ($Er(NO_3)_3$) were mixed in stoichiometric proportions and stirred continuously to homogenize. Alkaline medium (pH = 10) was created with ammonia solution that facilitated precipitation of nanoparticles. The precipitated nanoparticles were collected after decanting and cleaned thoroughly with ethanol. The resulting dried powder sample was annealed at 800 °C for 2 hours in air atmosphere to improve crystallinity. CPP technique was chosen as it can effectively incorporate dopants with improved homogeneity in nano-sized particles.

Characterisation

The X-ray powder diffraction (XRD) of the synthesized samples was examined on a Rigaku miniflex X-ray diffractometer using

the principle of Bragg Brentano Geometry, with Cu-Kα radiation (1.54 Å). The morphology of the synthesized undoped and Er^{3+} doped ZnO powder samples were inspected using a LEO 440 PC based digital scanning electron microscope (SEM) and FEI TECNAI F 30 TWIN, Transmission electron microscope (TEM). The photoluminescence (PL) characteristics were studied under a WITec Confocal fluorescence microscope (WITec 300M$^+$) with fluorescence mapping facility under sequential excitation of three diode lasers with wavelengths 375 nm, 980 nm and 1550 nm for realizing both down and up conversion properties of ZnO:Er^{3+} nanocrystals. A specific area of the sample was chosen under a 100× objective (NA 0.9) in the confocal microscope and fluorescence distribution was recorded under UV (375 nm, 10 mW) and IR diode lasers (980 nm, 300 mW and 1550 nm, 8 mW).

Acknowledgements

This present work was supported by the TAPSUN project under CSIR Solar Mission program of India. Authors thank Mr Satheesh Kumar of WITec Instruments for help in confocal measurements.

Notes and references

1 S. Ivanova, F. Pelle, A. Tkachuk, M. F. Joubert, Y. Guyot and V. P. Gapontev, *J. Lumin.*, 2008, **128**, 914–917.
2 Y. Bai, Y. Wang, K. Yang, X. Zhang, Y. Song and C. H. Wang, *Opt. Commun.*, 2008, **28**, 5448–5452.
3 Y. sun, H. Liu, X. Wang, X. Kong and H. Zhang, *Chem. Mater.*, 2006, **18**, 2726.
4 E. Rosa, P. Salas, H. Desirana, C. Angeles and R. Rodriguez, *Appl. Phys. Lett.*, 2005, **87**, 241912.
5 M. Kohls, M. Bonanni, L. Spanhel, D. Su and M. Giersig, *Appl. Phys. Lett.*, 2002, **81**, 3858.
6 S. Komuro, T. Katsumata, T. Morikawa, X. Zhao, H. Isshiki and Y. Aoyagi, *Appl. Phys. Lett.*, 2000, **76**, 3935.
7 A. G. Macedo, R. A. S. Ferreira, D. Ananias, M. S. Reis, V. S. Amaral, L. D. Carlos and J. Rocha, *Adv. Funct. Mater.*, 2010, **20**, 624.
8 J. Yang, C. Li, Z. Cheng, X. Zhang, Z. Quan, C. Zhang and J. Lin, *J. Phys. Chem. C*, 2007, **111**, 18148.
9 Q. Y. Zhang and X. Y. Huang, *Prog. Mater. Sci.*, 2010, **55**, 353.
10 U. Ozgur, Y. I. Alivov, C. Liu, A. Teke, M. A. Reshchikov, S. Dorgan, V. Avrutin, S. Jcho and H. Markoc, *J. Appl. Phys.*, 2005, **98**, 041301.
11 X. S. Wang, Z. C. Wu, J. F. Webb and Z. G. Liu, *Appl. Phys. A*, 2003, **77**, 561.
12 T. Dietl, H. Ohno, F. Matsukura, J. Cilbert and D. Ferrand, *Science*, 2000, **287**, 1019.
13 K. Jayanthi, S. Chawla, A. Joshi, Z. H. Khan and R. K. Kotnala, *J. Phys. Chem. C*, 2010, **114**, 18429.
14 X. Wang, X. Kong, Y. Yu, Y. Sun and H. Zhang, *J. Phys. Chem. C*, 2007, **111**, 15119–15124.
15 Y. Liu, Q. Yang and C. Xu, *J. Appl. Phys.*, 2008, **104**, 064701.
16 X. Wang, X. Kong, G. Shan, Y. Yu, Y. Sun, L. Feng, K. Chao, S. Lu and Y. Li, *J. Phys. Chem. B*, 2004, **108**, 18408–18413.
17 H. L. Lan, L. W. Yang, Y. X. Liu, Y. Y. Zhang and Q. B. Yang, *Opt. Mater.*, 2008, **31**, 338–341.
18 A. S. S. de Camargo, L. A. O. Nunes, J. F. Silva, A. C. F. M. Costa, B. S. Barros, J. E. C. Silva, G. F. desa and S. Alves Jr, *J. Phys.: Condens. Matter*, 2007, **19**, 2462209.
19 M. F. Joubert, S. Guy and B. Jacquier, *Phys. Rev. B: Condens. Matter Mater. Phys.*, 1993, **48**, 10031.
20 F. Auzel, *Chem. Rev.*, 2004, **104**, 139.
21 F. Vetrone, J. C. Boyer, J. A. Capobiano, A. Speghini and M. Bettinelli, *Appl. Phys. Lett.*, 2002, **80**, 1752.
22 X. Wang, X. Kong, Y. Yu, Y. Sun and H. Zhang, *J. Phys. Chem. C*, 2007, **111**, 15119–15124.
23 F. Xiao, R. Chen, Y. Q. Shen, Z. L. Dong, H. H. Wang, Q. Y. Zhang and H. D. Sun, *J. Phys. Chem. C*, 2012, **116**, 13458–13462.
24 N. Bloembergen, Solid state infrared quantum counters, *Phys. Rev. Lett.*, 1959, **2**, 84–85.
25 L. A. Diaz-Torres, E. De la Rosa-Cruz, P. Salas and C. Angeles-Chavez, *J. Phys. D: Appl. Phys.*, 2004, **37**, 2489–2495.
26 G. A. Kumar, M. Pokhrel and D. K. Sarda, *Mater. Lett*, 2012, **68**, 395–398.
27 Y. Qian, R. Wang, B. Zhag and B. Wang, *Opt. Lett.*, 2013, **38**, 19.
28 B. Lin, Z. Fu and Y. Jia, *Appl. Phys. Lett*, 2001, **79**, 945.
29 S. Singh, J. N. Divya Deepthi, B. Ramachandran and M. S. Ramachandra Rao, *Mater. Lett.*, 2011, **65**, 2930–2933.
30 S. Sharma, J. Shah, R. K. Kotnala and S. Chawla, *Electron. Mater. Lett.*, 2013, **9**, 615–620.